

1 **An emerging role of microplastics in the etiology of lung ground glass nodules**

2 Qiqing Chen<sup>1#,\*</sup>, Jiani Gao<sup>2#</sup>, Hairui Yu<sup>1</sup>, Hang Su<sup>2</sup>, Yan Yang<sup>1</sup>, Yajuan Cao<sup>3,4</sup>,

3 Qun Zhang<sup>1</sup>, Yijiu Ren<sup>2</sup>, Huahong Shi<sup>1</sup>, Chang Chen<sup>2\*</sup>, Haipeng Liu<sup>3,4\*</sup>

4

5 <sup>1</sup>State Key Laboratory of Estuarine and Coastal Research, East China Normal  
6 University, Shanghai 200241, China

7 <sup>2</sup> Department of Thoracic Surgery, Shanghai Pulmonary Hospital, Tongji University,  
8 Shanghai 200433, China

9 <sup>3</sup> Clinical and Translational Research Center, Shanghai Pulmonary Hospital, Tongji  
10 University, Shanghai 200433, China

11 <sup>4</sup> Central Laboratory, Shanghai Pulmonary Hospital, Tongji University, Shanghai  
12 200433, China

13

14 # These authors contributed equally to this work.

15 \*Correspondence should be addressed to Haipeng Liu ([haipengliu@tongji.edu.cn](mailto:haipengliu@tongji.edu.cn));

16 Chang Chen ([changchenc@tongji.edu.cn](mailto:changchenc@tongji.edu.cn)); or Qiqing Chen

17 ([chenqiqing@sklec.ecnu.edu.cn](mailto:chenqiqing@sklec.ecnu.edu.cn)).

18 **Abstract**

19 Pulmonary ground glass nodules (GGNs) have been increasingly identified in past  
20 decades and is becoming an important clinical dilemma in oncology. Meanwhile,  
21 humans persistently inhale microplastics which are dominant in the air. However, the  
22 retention of “non-self” microplastics in human lung and its correlation with pulmonary  
23 GGNs remains elusive. In this study, we firstly demonstrated the presence of  
24 microfibers and microplastics in human lung, with higher detection rates in GGNs in  
25 comparison to those in normal tissue. Moreover, both types and colors of microfibers  
26 in tumor were richer than those in normal tissues. Intriguingly, high risk of microfibers  
27 exposure predisposes the formation of pulmonary GGN. Further, increased roughness  
28 surface was observed in microfibers isolated in human lung, indicating the possible link  
29 of surface roughness to the formation of pulmonary GGN. Collectively, our findings  
30 reveal an emerging role of environmental microplastics exposure in the etiology of  
31 pulmonary GGN.

32

33 **One Sentence Summary**

34 The exposure of environmental microplastics is a risk factor of pulmonary GGN.

35

## 36 **Introduction**

37 Microplastic was firstly proposed as a marine environmental problem, but with its  
38 widespread occurrence in freshwater and estuary<sup>1-3</sup>, in land and mountains<sup>4, 5</sup>, and in  
39 glaciers and polar regions<sup>6, 7</sup>, microplastic pollution has become a global health issue  
40 and aroused some debates among scientists<sup>8-10</sup>. Recently, the pervasiveness of  
41 microplastics has also been verified in both indoor and outdoor air environments<sup>11</sup>, and  
42 the abundance of microplastics in the air is one order of magnitude higher than that in  
43 other media<sup>12</sup>. This means all living animals breathing with lungs (including humans)  
44 cannot escape the fate of inhaling microplastics.

45 Though the inhalation of mineral fiber such as asbestos has been widely recognized<sup>13</sup>,  
46 <sup>14</sup>, whereas pulmonary retention of nonmineral fibers including artificial fibrous  
47 microplastics or natural cotton fibers which are difficult to be degraded due to their  
48 stable structure remains unclear. The amount of microplastics humans take in through  
49 respiration may be much higher than other routes since microplastics are dominant in  
50 the air<sup>12</sup>. It has been predicted that the amount of microplastics inhaled by human body  
51 through breathing was dozens to hundreds per day<sup>15, 16</sup>. An early preliminary study  
52 reported the presence of fibers in human lung; however, there was a lack of detailed  
53 characterization of the fibers including the size and type, color and morphology<sup>17</sup>. Of  
54 note, there is no direct evidence to demonstrate what type and abundance of  
55 microplastics exist in lung tissue. In addition, whether the retention of microplastics  
56 and the long-term friction between microplastics and lung tissue are related to some  
57 respiratory diseases including lung cancer is largely unknown.

58 Pulmonary ground glass nodules (GGNs) are areas of lesions of homogenous density  
59 and with hazy increase in density in the lung field that does not obscure the broncho  
60 vascular structure as identified on low-dose computed tomography (LDCT)<sup>18-20</sup>. Their  
61 etiology is broad and the presumed significance is highly dependent on the underlying  
62 disease context<sup>21, 22</sup>. In addition to diagnostic techniques to increase the detection rate,  
63 the main causes of GGNs include genetic factors and gender factors<sup>23-26</sup>, but research  
64 suggests that environmental factors may affect the occurrence of GGNs or lung cancer<sup>24</sup>,  
65 <sup>27, 28</sup>. When exposed to asbestos, vinyl chloride, or other environmental factors, these

66 substances can be inhaled into the lungs to mount an immune response. The  
67 inflammatory response may form GGNs by wrapping, organizing or forming  
68 granulomas<sup>27</sup>. In addition, a long time exposure to a dusty environment without proper  
69 protection has been reported to impair lung function and cause GGNs<sup>28</sup>. Moreover,  
70 people who maintain smoking habits for a long time are more likely to cause GGNs<sup>24</sup>,  
71 <sup>29</sup>. The proportion of plastics produced and used in the current industrial civilization  
72 has increased year by year, leading to the existence of a large number of microplastics  
73 in the environment. This trend is consistent with the increasing incidence of GGN in  
74 recent years. In this study, we aimed to systematically detect and characterize the  
75 microplastics in GGNs and adjacent lung tissues, and analyzed the correlation of the  
76 presence of microplastics with the occurrence of GGNs.

77

## 78 **Results**

### 79 **Identification of microfibers in human lung tissue of pulmonary GGNs patients**

80 To detect whether microfibers are present in human lung tissues, we collected surgically  
81 dissected human lung tissues including GGNs and adjacent normal tissues in patients  
82 with pulmonary GGNs which are pathologically diagnosed. Pulmonary GGN can be  
83 observed in preinvasive lesions such as atypical adenomatous hyperplasia (AAH),  
84 adenocarcinoma in situ (AIS), or in malignancies such as minimally invasive  
85 adenocarcinoma (MIA), lepidic-predominant invasive adenocarcinomas (LPA)<sup>30</sup>. By  
86 using hydrogen peroxide digestion method, we successfully isolated microfibers from  
87 the lung tissues in both tumor (**Figure 1a-e**) and normal (**Figure 1f-h**) tissues. The most  
88 common types of microfibers are cotton (**Figure 1a**), rayon (**Figure 1b, g**), polyester  
89 (**Figure 1c, h**), denim (**Figure 1f**), and the representative examples are presented.  
90 Besides, we also found some kind of microfibers that rarely found in water or soil, such  
91 as phenoxy resin (**Figure 1d**) and chipboard (**Figure 1e**). There was no obvious  
92 difference in gross morphology between the tumor and normal groups.

93

### 94 ***In situ* detection of microfibers in human lung tissue of pulmonary GGNs patients**

95 To further demonstrate the presence of microfibers in human lung, we employed the

96 Laser Direct Infrared (LDIR) method to detect the microfibers in the lung tissue slice  
97 from pulmonary GGNs patients *in situ*. By analyzing cryo-sectioned slices, we  
98 successfully observed the presence of a microfiber (width 24  $\mu\text{m}$ , length 887  $\mu\text{m}$ ) in the  
99 lung tissue slice by microscopy observation with both visible light (**Figure 2a, d**) and  
100 infrared spectrum (**Figure 2b, c**). The infrared absorption spectrum revealed that the  
101 composition of the microfiber was cellulose (**Figure 2e**). This was further consolidated  
102 by the collected signals with the specific cellulose characteristics (**Figure 2f**), which  
103 indicates that this fiber component is indeed cellulose and is different from the  
104 surrounding components. As the characteristic signal intensities of this microfiber were  
105 uneven at different regions (**Figure 2f**), we suppose that this microfiber should be  
106 embedded in the tissue. We therefore for the first time provide solid *in situ* evidence to  
107 support the presence of microfiber in human lung tissue.

108

### 109 **Higher detection rate of microfibers in the GGNs**

110 To understand whether the presence of microfibers is associated with the occurrence of  
111 GGNs, we further compared the frequency of the detected microfibers in the GGNs and  
112 adjacent normal lung tissues. In 50 pairs of samples, microfibers have been found in 29  
113 tumor and 23 normal tissues (**Figure 3a**), in the female subgroup, the detection rates of  
114 microplastics in tumor and normal tissues were different (**Figure 3c-3d**), thus, the  
115 positive detection rates were 58% and 46% for tumor and normal tissues, respectively.  
116 Moreover, a total of 38 microfibers were detected in tumor tissues, accounting for 58.46%  
117 of the total detected microfibers; while 27 microfibers were detected in normal tissues,  
118 accounting for 41.54% (**Figure 3b**). Among the detected microfibers, 24 were  
119 microplastics, constituting 36.92% of the total microfibers (**Figure 3b**). Sixteen  
120 microplastics were detected in the tumor tissues, which was twice than that of the  
121 normal tissues (**Figure 3b**). Taken together, in comparison to that in normal lung tissues,  
122 the detection rate of microfibers or microplastics in GGNs was significantly higher,  
123 indicating a possible link of the presence of microfibers to the occurrence of GGNs.

124

125

## 126 **Characterization of microfibers in the lung tissues of pulmonary GGN patients**

127 Next, we checked the characteristics including width, length, type and color of  
128 microfibers isolated in human lung tissues. The average values of length ( $1.45\pm 0.98$   
129 mm) and width ( $35.74\pm 21.09$   $\mu\text{m}$ ) of microfibers in tumor tissues are slightly higher  
130 than those in the normal ( $1.38\pm 0.96$  mm for length, and  $32.81\pm 16.91$   $\mu\text{m}$  for width), but  
131 there is no significant difference between them (**Figure 4a**). Additionally, both the  
132 length of microplastics in tumor ( $1.75\pm 0.79$  mm) and normal ( $1.49\pm 0.96$  mm) tissues,  
133 and the width of microplastics in tumor ( $34.29\pm 18.60$   $\mu\text{m}$ ) and normal ( $34.15\pm 17.91$   
134  $\mu\text{m}$ ) tissues are quite similar (**Figure 4a**). Moreover, microfibers detected in the lungs  
135 were mainly  $>1000$   $\mu\text{m}$  in length, with 63% for microfiber and 50% for microplastic in  
136 tumor tissue, 48% for microfiber and 63% for microplastic in normal tissue (**Figure**  
137 **S1a-b**). The width of microfiber mainly falls in  $<30$   $\mu\text{m}$  in both tumor and normal  
138 tissues, accounting 47.37% and 51.85%, respectively. However, microplastic widths  
139 have the highest proportion of 30-50  $\mu\text{m}$  in tumor tissue, accounting 56.25%, while the  
140 highest proportions of  $<30$  and 30-50 in normal tissue are both 37.5% (**Figure S1c-d**).

141

142 Moreover, multiple types of microfibers were detected in the lung. The dominant type  
143 of microfibers is cotton which accounts for 39.47% in tumor and 51.85% in normal  
144 tissues, respectively. Rayon ranks the second and constitutes 26.32% and 18.52% of  
145 tumor and normal tissues, respectively. The third is polyester, which accounts for 10.53%  
146 of tumor and 11.11% of normal tissues. Moreover, 10 kinds of microfibers are detected  
147 in tumor, which is more abundant than normal tissues (6 kinds) (**Figure 4b**). The colors  
148 of microfibers, whether in tumor or normal tissues, are mainly purple and blue with  
149 different shades, and a small amount of transparent and yellow microfibers are detected.  
150 There are more reddish microfibers in normal tissues (**Figure 4c**).

151

## 152 **Characterization of microfibers in matched tumor and normal lung tissues**

153 Parameters commonly used to describe the characteristics of microfibers including  
154 polymer composition, size, color, density, shape<sup>31</sup>. To further make clear which  
155 characteristic of microfibers may be responsible for the occurrence of GGNs, we also

156 conducted matched samples comparison for the case that microfibers were detected in  
157 both tumor and normal tissues of the same patient. Although the mean values of width  
158 and length in tumor are higher than those in normal tissues, the difference is not  
159 significant (**Figure 5a**), and only one tenth of the colors and one third of the fiber  
160 composition types are the same in matched tumor and normal tissues (**Figure 5b-c**).

161

## 162 **High risk of microfibers exposure correlates with the occurrence of pulmonary** 163 **GGNs**

164 To further study the correlation of microfibers with the occurrence of GGNs, we  
165 examined the factors contributing to the accumulation of microfibers in the GGN tumor  
166 tissues. Chi-square test revealed that microfibers are more likely to be detected in the  
167 tumor tissue if one has a history of high microfiber exposure risk in life or work, with  
168 a microfiber detection rate reaches 72% (**Figure 6a**). However, this phenomenon was  
169 not found in the normal tissue, and the detection rate was 45% (**Figure 6a**). This  
170 suggests that the exposure to microfibers may lead to the accumulation of microfibers  
171 in the lung, which finally contributes to the formation of GGNs.

172 Initially, a sex-specific difference in incidence of lung cancer has been reported, women  
173 are most likely developing GGN<sup>32, 33</sup>. We next examined whether gender is related to  
174 the detection rate of microfibers in the tumor or normal tissue of the lung. The  
175 microfiber detection rate of the female (n=34) in either tumor (61.76%) or normal  
176 (47.06%) tissues is higher than that of the male (n=16, 53.33% and 40.00%,  
177 respectively), but there is no significant difference between the two genders according  
178 to the chi-square test result (**Figure 6b**).

179 In addition, according to the age classification of lung cancer epidemiology, we found  
180 that with the increase of age, the content of microfiber in lung tissue gradually increased  
181 (**Figure 6c**). Importantly, the amount of microfibers in normal tissue is significantly  
182 increased with age; however, the magnitude of microfibers in tumor tissues of patients  
183 with GGN of all ages are high and not significantly different (**Figure 6c**). Of note,  
184 microfibers were identified in the tumor tissue but not in the any normal tissue of  
185 pulmonary GGO patients aged from 25-44 (n=6), indicating that inhalation and

186 accumulation of microfibers in the young people may be a risk factor for the occurrence  
187 of GGN.

188

### 189 **Microfibers isolated from lung tissues exhibit high surface roughness**

190 We further characterize the microfibers in human lung tissues by scan electron  
191 microscope, the data demonstrate that there are numerous wear and gullies on  
192 microfibers as detected by their typical main body structure (**Figure 7a, c, e**) and local  
193 surface morphology (**Fig. 7b, d, f**). Of note, little attention has been paid to the index  
194 of surface roughness. This kind of morphology is different from that found in the  
195 atmospheric fallout in Shanghai, as we find that there are both worn or unworn  
196 microfibers in the air (**Figure S2**), which may be related to their aging degree in the  
197 environment. Besides, our data confirmed that the sampling, digestion and  
198 identification processes would not be the cause of surface wear (**Figure S3**). Of note,  
199 microfibers in both tumor and normal tissues exhibited a higher roughness value  
200 ( $Ra=0.90\pm 0.84\ \mu\text{m}$ , and  $0.79\pm 0.43\ \mu\text{m}$ , respectively) than those in air ( $Ra=0.38\pm 0.22$   
201  $\mu\text{m}$ ) ( $p=0.183$ ) (**Figure 7g**), and obvious rougher surface of microfibers in lung tissues  
202 than that in the air can be observed (**Figure 7h-k**). Moreover, energy-dispersive X-ray  
203 spectroscopy (EDS) revealed that microfibers isolated in the lung did not harbor  
204 obvious heavy metal residues (**Figure S4**). Therefore, it is very possible that the surface  
205 roughness of microfibers was formed after entering the lungs, formed during  
206 microfibers' long-term interaction with the lungs.

207

### 208 **Discussion**

209 The interrogation of the correlation of microplastics with diseases is an emerging field.  
210 The presence of microplastics in human tissues including gastrointestinal tract and  
211 placenta<sup>34, 35</sup> has been previously reported. In this study, we provided solid evidence  
212 demonstrating the presence of microplastics in human lung tissues. Preliminary data  
213 demonstrated a higher detection rate of microplastics in the GGNs in comparing to the  
214 adjacent normal lung tissues. Moreover, the history of exposure to microfibers  
215 correlates with the occurrence of GGNs, which implicates an involvement of microfiber



216 exposure in the etiology of GGNs.

217

### 218 **High abundance of microfibers and microplastics in human lung**

219 The average wet weight of tissue samples used in this study is  $44\pm 32$  mg, with  
220  $0.65\pm 0.70$  microfiber/sample detected. Thus, the predicted microfiber abundance in a  
221 whole human lung can reach 11,818 microfiber/lung (calculated as 800 g). As the  
222 content of microplastics accounting for 45% and 33% in normal and tumor tissues  
223 respectively, it is predicted that microplastic abundance in a whole lung can be 3,900-  
224 5,318 microplastic/lung. In our study, we found that the detection rate of microfibers in  
225 normal tissue is significantly increased with age; however, the detection rates of  
226 microfibers in patients with GGN of all ages are equivalent and high. This phenomenon  
227 indicates that microfibers may affect the occurrence of GGN after reaching the  
228 cumulative threshold.

229

230 The microfibers detected in the lungs were mainly ranged from 1000 to 5000  $\mu\text{m}$  in  
231 length. This is different from the length distribution of microfibers in mountainous areas  
232 or medium-sized cities. For instance, a recent study found only around 11% of  
233 atmospheric deposited microfibers ranged in  $>1000$   $\mu\text{m}$  collected from a remote  
234 mountain catchment (French pyrenes)<sup>36</sup>. In the medium-sized Dongguan city,  
235 atmospheric fallout microfibers longer than 1200  $\mu\text{m}$  constituted around 44%<sup>37</sup>.  
236 However, our microplastics distribution is close to the atmospheric microplastics  
237 distribution in an urban area of Paris, with 49% fell in the range of 1000-5000  $\mu\text{m}$ <sup>38</sup>.  
238 This suggests that large cities may have a high proportion of long fibers in the air than  
239 medium-sized cities or remote areas. Of note, since our patients come from different  
240 cities and rural areas in China, the high percentage of long fibers in lungs may be  
241 because the longer inhaled microfibers may be easily entangled in lungs and difficult  
242 to be dispelled.

243

244 In addition to artificial fibrous microplastics, the cotton microfibers occupied a high  
245 proportion (39% in tumor tissue and 52% in normal tissue). Due to the not easily

246 biodegradable nature, these cotton microfibers should have similar toxic effects as  
247 microplastics, if the indirect toxic effects of microplastics by releasing additives is not  
248 taken into account.

249

250 Most of the pulmonary microfibers probably come from indoor or outdoor air exposure,  
251 because the types of microfibers in lung tissue are highly similar to those found in the  
252 atmospheric fallout<sup>11</sup>, with the highest content being cotton, rayon and polyester.  
253 Previous studies have highlighted the presence of synthetic fibers in the lung tissue of  
254 workers in the textile industry, showing cases of respiratory irritation<sup>39, 40</sup>. The  
255 inhalability of a particle is size and shape dependent, as only the smallest particles  
256 below 5  $\mu\text{m}$  and fibrous particles seem to be able to be deposited in the deep lung. Even  
257 though most of the bigger particles (inhalable particles) are subjected to mucociliary  
258 clearance in the upper airways, some of them can escape this mechanism and also be  
259 deposited in the deep lung. These particles (especially the longer fibers) tend to avoid  
260 clearance and show extreme durability in physiological fluids, likely persisting and  
261 accumulating when breathed in. This may be the reason why the proportion of long  
262 fibers (>1000  $\mu\text{m}$ ) in lung tissue (48-63%, **Figure S1**) is much higher than that in urban  
263 (44% for >1200  $\mu\text{m}$ )<sup>37</sup> or mountainous air (11% for >1000  $\mu\text{m}$ )<sup>36</sup>. Previous studies  
264 report microfiber lengths merely. In this study, we firstly report the microfiber width  
265 (or diameter) dimension of microfibers in lung tissues, which is vital factor regulating  
266 the deposition of microfibers in the respiratory tract<sup>41</sup>.

267

268 The morphology of the inhaled fibers (e.g., air pollutants and microplastics) may affect  
269 their aerodynamic properties<sup>42, 43</sup> which thereby finally modulate their ability to deposit  
270 in the distal pulmonary acinar airways as a result of varied width. Width is the main  
271 factor that determines whether or where in the respiratory tract that a microfiber can  
272 deposit<sup>41</sup>. Our results suggest that 13-125  $\mu\text{m}$  wide microfibers/microplastics can reach  
273 lung tissues, with a mean width value of  $\sim 30$   $\mu\text{m}$ . Once deposited, fiber length is the  
274 main factor that determines whether a microfiber can be effectively cleared<sup>41</sup>. Such  
275 elongated fibers (a mean value of  $\sim 1.4$  mm) tend to align with respiratory airflows, due

276 to higher drag forces that resist sedimentation under gravity, and thus present a special  
277 clearance challenge for the lung compared with spheres of equivalent mass<sup>44</sup>. The thin,  
278 elongated shape of microfibers also affects clearance rates, enabling them to get  
279 entrained into the epithelial layer while inhibiting engulfment by macrophages<sup>41, 45</sup>.  
280 Combined with a high surface-to-volume ratio compared to spheres of equivalent mass,  
281 such characteristics render non-spherical particles, and fibers in particular, promising  
282 candidates to be delivered to the deep lungs, which is supported by the finding that the  
283 microfibers identified in the lung are elongated in this study. Furthermore, the surface-  
284 to-volume ratio, hydrophobicity, size, and other properties of the microfibers can  
285 enhance their ability to attach heavy metal, increasing damage to the pulmonary  
286 immune microenvironment.

287

### 288 **Microfibers and the etiology of GGNs**

289 Generally, when microfibers enter the respiratory system, the lung tissue has two main  
290 ways to dispel them. If microfibers deposited on the surface of respiratory mucosa, they  
291 can be excreted out of the respiratory tract by coughing or mucociliary escalator<sup>46</sup>. If  
292 microfibers reached the alveolar region, macrophages in the alveoli could remove the  
293 microfibers through phagocytosis, migration, or lymphatic transportation  
294 mechanisms<sup>47</sup>. Macrophages in alveoli often have high clearance efficiency for  
295 particles larger than 1  $\mu\text{m}$ , thus microfibers at the micro-sized level are theoretically  
296 difficult to remain in lung tissue<sup>48</sup>. However, if the lung is continuously exposed to  
297 microfibers for a long time, it may cause excessive secretion of chemokines in the lung,  
298 thus destroying the normal chemotactic gradient, and may result in macrophages  
299 containing ingested microfibers resting in the alveolar space. Or if macrophages engage  
300 in “frustrated” phagocytosis for microfibers, digestive enzymes and other cellular  
301 contents will be spilled into the alveolar space, and this may mount innate immune  
302 responses which drive the sterile inflammation, fibrosis and other malignancies in the  
303 lung<sup>43</sup>, which thereby participate in the formation of GGNs and other inflammatory  
304 respiratory diseases. . The ingestion of microfibers by macrophage may mount innate  
305 immune responses which drive the sterile inflammation in the lung, which thereby

306 participate in the formation of GGNs and other inflammatory respiratory diseases.  
307 Moreover, the interaction between vitreous particles/fibers and cells may lead to lung  
308 inflammation via intracellular messengers and cytotoxic factors which are released, and  
309 then cause secondary genotoxicity due to the continuous formation of reactive oxygen  
310 species<sup>47, 49</sup>.

311

312 Increasing evidence demonstrated that microfiber carry bacteria/virus<sup>50</sup>, which may  
313 play an important role in their interaction with the host. Intriguingly, compared to  
314 normal tissue, GGNs harbored a distinct lung bacterial community structure, with  
315 significantly increasing Firmicutes and Bacteroidetes<sup>51-53</sup>. Even though there is no  
316 report about the biofilm community on airborne microplastics, but the biofilm  
317 community structures on microplastics are more affected by morphology/surface  
318 texture rather than polymer composition<sup>54</sup>. Therefore, we can further perform  
319 microbiota analysis on GGNs and normal tissues containing microfibers to further  
320 reveal the influence of microfiber on the lung microbiota. It's tempting to speculate  
321 whether the microbes carried along by microfibers play a role in shaping the specific  
322 structure of microbiota in GGN. The microbiota analysis of GGNs and normal tissues  
323 that contain or free of microfibers will facilitate to understand the role of microfiber in  
324 modulating lung microbiota.

325

326 Moreover, airborne microplastic is an ideal vehicle for carrying micropollutants  
327 adsorbed to their hydrophobic surface, especially when related to urban environments.  
328 Recent studies performed using pre-diagnostic serum samples suggest that  
329 environmental exposure to micropollutants play an important role in the development  
330 of a series of cancers including lung cancer, prostate cancer, breast cancer, liver cancer  
331 and acute myeloid leukemia<sup>55-58</sup>. It's therefore reasonable to speculate that microplastic  
332 may affect the occurrence of GGNs by delivering micropollutants which exerts toxic  
333 effect on the host. Of note, in addition to the adsorbed pollutants, microplastics may  
334 also contain unreacted monomers, additives, dyes, and pigments which could lead to  
335 adverse health effects<sup>59, 60</sup>. Though no heavy metal residue was found here by EDS

336 **(Figure S4)**, which may be due to the high detection limit of this method. However,  
337 there is no doubt that the high hydrophobicity and adsorption properties of  
338 microplastics will lead to the possibility of carrying pollutants into lung tissues, which  
339 needs further attention in the future.

340

#### 341 **Surface roughness—a characteristic of microfibers awaits attention**

342 Parameters commonly used to describe the characteristics of microfibers include  
343 polymer composition, size, color, density, shape, etc.; whereas little attention is paid to  
344 the index of surface roughness. Here we found all microfibers had obvious surface wear  
345 in both normal or tumor tissues. This kind of morphology is different from that found  
346 in the air, which shows both worn or unworn morphology and may be related to their  
347 aging degree in the environment. Besides, our pilot experiment confirmed that the  
348 increased surface roughness is not caused by the sampling, digestion and identification  
349 processes. It's therefore highly likely that the surface roughness of microfibers was  
350 formed after entering the lungs. Some environmental processes, such as mechanical  
351 erosion by wind, water, or sand, UV radiation, biodegradation will increase the  
352 roughness of microplastics<sup>5, 61, 62</sup>. However, there is no report about the increase of  
353 roughness after microfibers/microplastics enter tissues. We believe this is the first report  
354 of the serious roughness phenomenon of microfibers in human tissues.

355 Little is known about the consequence of enhanced surface roughness to its interaction  
356 with the host. It would be interesting to check whether such characteristic of microfibers  
357 modulates its interaction with alveolar macrophages in multiple processes such as  
358 phagocytosis, recognition and mounting of immune responses. The types of cell death  
359 including apoptosis and necrosis in response to exogenous stimulation often show  
360 distinct effect on the outcome of diseases<sup>63</sup>. It would be fascinating to take the surface  
361 roughness as an important characteristic of microfibers into account in study its role in  
362 modulating the fate of macrophages and shaping of the microenvironment, which may  
363 constitute a new direction in future research of microfiber-host interaction. The  
364 technological advancement in acquisition of nano-scale microfibers will also promote  
365 the research on microfiber-host interaction.

## 366 **Microfibers link pulmonary GGN to occupational disease**

367 Some occupational diseases may be related to long-term exposure to microfibers or  
368 microplastics. The “fiber-drawing workers” experienced a statistically significant  
369 excess in mortality from lung cancer<sup>39</sup>. Some of the nylon flock exposed workers had  
370 abnormal chest radiographs five-fold than non-exposed ones<sup>40</sup>. In the current study, we  
371 found that the microfibers significantly elevated in the normal lung tissues of  
372 pulmonary GGN patients with the increase of age. This phenomenon pinpoints the  
373 importance of the cumulative threshold of microplastics present in the lung in affecting  
374 the occurrence of GGN. Moreover, the data demonstrated that the long-term exposure  
375 to microfibers or microplastics is a risk factor for the formation of GGNs, indicating  
376 that it’s important for the clinicians to consider occupational exposure in the diagnosis  
377 of pulmonary GGNs. Our work also suggests that it’s important to perform the routine  
378 health examination in those people who have high risk to expose to microplastics,  
379 especially in the young people.

380

## 381 **Methods**

### 382 **Clinical samples**

383 Patients who underwent VATS lobectomy/sublobectomy for NSCLC in Shanghai  
384 Pulmonary Hospital between January 2020 and December 2020 were reviewed.  
385 Included in our studies were lung specimens with ground glass nodule (GGN). Tissue  
386 wet weight ( $0.043 \pm 0.031$  g,  $n = 100$ ). All patients received preoperative workups,  
387 including chest computed tomography (CT), brain magnetic resonance imaging (MRI),  
388 whole-body PET-CT and bronchoscopy. If N2 disease was suspected in PET-CT,  
389 endobronchial ultrasound was conducted to rule it out. This study was conducted in  
390 accordance with the principles of the Declaration of Helsinki. The study protocol was  
391 approved by the ethics committee of the Shanghai Pulmonary Hospital (IRB NO. K21-  
392 020), and informed consent from individual patients was waived for this retrospective  
393 analysis.

394

## 395 **Sample Digestion**

396 Each lung tissue was transferred by stainless tweezers into a 40-mL glass tube, and 30  
397 mL of H<sub>2</sub>O<sub>2</sub> (30 %, v/v) were added. The tubes were then incubated at 65°C and 80 rpm  
398 for 72 h for digestion. Afterwards, the digestate was filtered through a 5 µm filter  
399 membrane (MCE, Millipore SMWP04700) and the filter membrane was stored in a dry  
400 glass petri dish for further observation and identification. All containers and tools were  
401 rinsed with Milli-Q water three times before use to avoid microfiber contamination.  
402 Procedural controls were conducted in parallel after the collection of lung tissues and  
403 throughout the following experiments.

## 404 **Observation and Identification of Microfibers**

405 We used a Carl Zeiss Discovery V8 Stereo microscope (Micro Imaging GmbH,  
406 Germany) and an AxioCam digital camera to observe and photograph the substances  
407 on the surface of the membrane. Then, the composition of the suspected microfibers  
408 (including microplastics) was identified with µ-FT-IR (Nicolet iN 10, Thermo Fisher)  
409 under the transmission mode. A resolution of 4 cm<sup>-1</sup> with a 16<sup>-s</sup> scan time was chosen  
410 for data collection. All spectra were matched with our modified database and the result  
411 was accepted only when the matching index ≥ 70%. The Image J software (NIH Image)  
412 was used to measure the basic parameters (i.e. length, width and color) of fibers and  
413 fragments. Compare the colors of fibers and fragments with Pantone International Color  
414 Card by visual inspection, and express their colors with International standard color  
415 numbers and color scales.

## 416 **SEM/EDS analysis**

417 To understand the surface morphology and elemental composition of microfibers or  
418 fragments from lung tissues, twelve representative samples (6 each of normal and tumor  
419 tissues) were studied using scanning electron microscope (SEM) (S4800) and Cryo-  
420 SEM (Lecia EM ICE, AFS2, FC7, TIC3X \*, German) combined with energy-dispersive  
421 X-ray spectroscopy (EDS).

422 To confirm the effect of transportation, digestion, observation and identification

423 processes on the surface morphology of microfibers, we conducted a pilot experiment  
424 by preparing two kinds of microfibers with the highest detection rate in our study  
425 (cotton and crayon) from the laboratory before and after all the above processes.  
426 Microfibers collected from indoor air in Shanghai were also collected for observation,  
427 including nine microfibers (3 each of cotton, rayon and polyester).

428 Microfibers were fixed on double-sided adhesive carbon tabs on the sample stage and  
429 spray gold. High resolution imaging was carried out by field emission SEM working at  
430 3.0 KV and 15  $\mu$ A, and the samples were taken at a magnification of 5.00 K. Qualitative  
431 elemental composition of six selected samples were determined by EDS working at  
432 20.0kV and 20  $\mu$ A.

#### 433 **Microfiber surface roughness measurement**

434 The surface roughness profile of microfibers was obtained by using a three-dimensional  
435 white light interferometry optical profiler Bruker Contour GT-K. The surface of  
436 middle area of microfibers were selected for detection. The entire profile data points  
437 were recorded, and the roughness average (Ra) of the absolute values of profile heights  
438 over a given area<sup>64</sup> were calculated for each microfiber to evaluate their roughness,  
439 according to the standard method ASME B46.1-2009<sup>65</sup>.

#### 440 ***In situ* Observation of Microfibers**

441 The surgical lung tissues were cut into 30  $\mu$ m slices and left untreated or treated with  
442 proteinase K (20 mg/mL) at 37 °C for 10 min. Each sample was then fixed to the  
443 microscope slide of dimension 25 mm  $\times$  75 mm using optical adhesive. To identify the  
444 *in situ* presence of microfibers in lung tissues, we used the Agilent 8700 Laser Direct  
445 Infrared (LDIR) Chemical Imaging System, equipped with a quantum cascade laser  
446 (QCL) source and a single point Mercury Cadmium Telluride (MCT) detector, at  
447 Agilent Technologies Application Laboratory in Shanghai, China. Briefly, the slides  
448 were firstly put in the LDIR system, and the height of samples were automatically  
449 identified and the tissue sections were focused. Then, the LDIR analyzer rapidly  
450 scanned the sample area at 1200  $\text{cm}^{-1}$  with 20- $\mu$ m resolution, and found and targeted



451 areas containing suspect microfibers. Next, the targeted areas were enlarged and  
452 scanned with a fine resolution of 10  $\mu\text{m}$ . Finally, the spectrum data were collected, and  
453 microfiber matching results were provided by conducting a library searching.

#### 454 **Clinical indices**

455 Through interviews with patients, we obtained first-hand information about the history  
456 of microfiber exposure of the patients. (1) We define people who smoke or have had a  
457 history of smoking as high risk of microfiber exposure, because cigarette butts contain  
458 various types of microfibers<sup>66</sup> and could be inhaled in with the smoke. (2) We define  
459 people who have a high cooking frequency at home as high risk of microfiber exposure,  
460 because long time cooking and other housework will increase the microfiber exposure<sup>67</sup>,  
461 <sup>68</sup>. (3) We also inquired about the occupational background of the patients, and listed  
462 the patients who work in shoe factories, farms, construction sites, garbage cleaning, etc.  
463 as having high risks of microfiber exposure.

#### 464 **Statistical Analysis**

465 The microfiber or microplastic amount differences among tumor and normal tissue  
466 groups were evaluated by paired *t*-test. The microfiber exposure history and gender  
467 effects on the microfiber or microplastic detection results were evaluated by Chi-square  
468 test. All the above analyses were performed with SPSS (SPSS, version 20.0). Figures  
469 were plotted with GraphPad Prism (GraphPad, version 8.0).

470

#### 471 **References**

- 472 1. Li, J. Y.; Liu, H. H.; Chen, J. P., Microplastics in freshwater systems: a review on occurrence,  
473 environmental effects, and methods for microplastics detection. *Water Research* **2018**, *137*, 362-374.
- 474 2. Leslie, H. A.; Brandsma, S. H.; van Velzen, M. J. M.; Vethaak, A. D., Microplastics en route: field  
475 measurements in the Dutch river delta and Amsterdam canals, wastewater treatment plants, North Sea  
476 sediments and biota. *Environment International* **2017**, *101*, 133-142.
- 477 3. Rochman, C. M., Microplastics research—from sink to source. *Science* **2018**, *360*, (6384), 28-29.
- 478 4. Zhang, G. S.; Liu, Y. F., The distribution of microplastics in soil aggregate fractions in southwestern  
479 China. *Science of the Total Environment* **2018**, *642*, 12-20.

- 480 5. Napper, I.; Davies, B.; Clifford, H.; Elvin, S.; Koldewey, H.; Mayewski, P.; Miner, K.; Potocki, M.;  
481 Elmore, A.; Gajurel, A., Reaching new heights in plastic pollution—preliminary findings of microplastics  
482 on Mount Everest. *One Earth* **2020**, *3*, 621-630.
- 483 6. Obbard, R. W.; Health, Microplastics in polar regions: the role of long range transport. *Current*  
484 *Opinion in Environmental Science Health* **2018**, *1*, 24-29.
- 485 7. Ambrosini, R.; Azzoni, R. S.; Pittino, F.; Diolaiuti, G.; Franzetti, A.; Parolini, M., First evidence of  
486 microplastic contamination in the supraglacial debris of an alpine glacier. *Environmental Pollution* **2019**,  
487 *253*, 297-301.
- 488 8. Galloway, T. S., Micro- and nano-plastics and human health. In *Marine anthropogenic litter*,  
489 Springer, Cham: 2015; pp 343-366.
- 490 9. Rochman, C. M.; Browne, M. A.; Halpern, B. S.; Hentschel, B. T.; Hoh, E.; Karapanagioti, H. K.;  
491 Rios-Mendoza, L. M.; Takada, H.; Teh, S.; Thompson, R. C., Classify plastic waste as hazardous. *Nature*  
492 **2013**, *494*, (7436), 169-171.
- 493 10. Kramm, J.; Völker, C.; Wagner, M., Superficial or substantial: Why care about microplastics in the  
494 anthropocene? *Environmental Science & Technology* **2018**, *52*, (6), 3336-3337.
- 495 11. Zhang, Q.; Zhao, Y.; Du, F.; Cai, H.; Shi, H., Microplastic fallout in different indoor environments.  
496 *Environmental Science & Technology* **2020**, *54*, (11), 6530-6539.
- 497 12. Zhang, Q.; Xu, E. G.; Li, J. N.; Chen, Q. Q.; Ma, L. P.; Zeng, E. Y.; Shi, H. H., A review of  
498 microplastics in table salt, drinking water, and air: direct human exposure. *Environmental Science &*  
499 *Technology* **2020**, *54*, (7), 3740-3751.
- 500 13. Spasiano, D.; Pirozzi, F., Treatments of asbestos containing wastes. *Journal of Environmental*  
501 *Management* **2017**, *204*, 82-91.
- 502 14. Yang, X.; Yan, Y.; Xue, C.; Du, X.; Ye, Q., Association between increased small airway obstruction  
503 and asbestos exposure in patients with asbestosis. *Clinical Respiratory Journal* **2018**, *12*, (4), 1676-1684.
- 504 15. Vianello, A.; Jensen, R. L.; Liu, L.; Vollertsen, J., Simulating human exposure to indoor airborne  
505 microplastics using a Breathing Thermal Manikin. *Scientific Reports* **2019**, *9*, (1), 1-11.
- 506 16. Prata, J. C.; da Costa, J. P.; Lopes, I.; Duarte, A. C.; Rocha-Santos, T., Environmental exposure to  
507 microplastics: an overview on possible human health effects. *Science of the Total Environment* **2020**, *702*,  
508 134455.
- 509 17. Pauly, J. L.; Stegmeier, S. J.; Allaart, H. A.; Cheney, R. T.; Zhang, P. J.; Mayer, A. G.; Streck, R. J.,

- 510 Inhaled cellulosic and plastic fibers found in human lung tissue. *Cancer Epidemiology Biomarkers &*  
511 *Prevention* **1998**, 7, (5), 419-428.
- 512 18. Team, N. L. S. T. R., Reduced lung-cancer mortality with low-dose computed tomographic  
513 screening. *New England Journal of Medicine* **2011**, 365, (5), 395-409.
- 514 19. Lee, H. Y.; Lee, K. S., Ground-glass opacity nodules: histopathology, imaging evaluation, and  
515 clinical implications. *Journal of Thoracic Imaging* **2011**, 26, (2), 106-118.
- 516 20. Pedersen, J. H.; Saghir, Z.; Wille, M. M. W.; Thomsen, L. H.; Skov, B. G.; Ashraf, H., Ground-glass  
517 opacity lung nodules in the era of lung cancer CT screening: radiology, pathology, and clinical  
518 management. *Oncology* **2016**, 30, (3), 266-274.
- 519 21. Fukui, T.; Mitsudomi, T., Small peripheral lung adenocarcinoma: clinicopathological features and  
520 surgical treatment. *Surgery Today* **2010**, 40, (3), 191-198.
- 521 22. Godoy, M. C.; Naidich, D. P., Subsolid pulmonary nodules and the spectrum of peripheral  
522 adenocarcinomas of the lung: recommended interim guidelines for assessment and management.  
523 *Radiology* **2009**, 253, (3), 606-622.
- 524 23. Ichinose, J.; Kohno, T.; Fujimori, S.; Harano, T.; Suzuki, S.; Fujii, T., Invasiveness and malignant  
525 potential of pulmonary lesions presenting as pure ground-glass opacities. *Annals of Thoracic*  
526 *Cardiovascular Surgery* **2014**, 20, (5), 347-352.
- 527 24. Kobayashi, Y.; Ambrogio, C.; Mitsudomi, T., Ground-glass nodules of the lung in never-smokers  
528 and smokers: clinical and genetic insights. *Translational Lung Cancer Research* **2018**, 7, (4), 487.
- 529 25. Zhang, Y.; Deng, C.; Fu, F.; Ma, Z.; Wen, Z.; Ma, X.; Wang, S.; Li, Y.; Chen, H., Excellent prognosis  
530 of patients with invasive lung adenocarcinomas intraoperatively misdiagnosed as AAH/AIS/MIA by  
531 frozen section. *Chest* **2021**, in Press.
- 532 26. Kim, S. S.; Bharat, A., Commentary: Video assisted thoracoscopic surgery vsersus robotic assisted  
533 surgery: are we asking the right question? *The Journal of Thoracic and Cardiovascular Surgery* **2020**,  
534 160, (5), 1374-1375.
- 535 27. Meyer, M.; Vliegenthart, R.; Henzler, T.; Buergy, D.; Giordano, F. A.; Kostrzewa, M.; Rathmann,  
536 N.; Brustugun, O. T.; Crino, L.; Dingemans, A.-M. C., Management of progressive pulmonary nodules  
537 found during and outside of CT lung cancer screening studies. *Journal of Thoracic Oncology* **2017**, 12,  
538 (12), 1755-1765.
- 539 28. He, Y.-T.; Zhang, Y.-C.; Shi, G.-F.; Wang, Q.; Xu, Q.; Liang, D.; Du, Y.; Li, D.-J.; Jin, J.; Shan, B.-

- 540 E., Risk factors for pulmonary nodules in north China: a prospective cohort study. *Lung Cancer* **2018**,  
541 *120*, 122-129.
- 542 29. Pinsky, P.; Gierada, D. S., Long-term cancer risk associated with lung nodules observed on low-  
543 dose screening CT scans. *Lung Cancer* **2020**, *139*, 179-184.
- 544 30. Lee, H. J.; Lee, C. H.; Jeong, Y. J.; Chung, D. H.; Goo, J. M.; Park, C. M.; Austin, J. H. M.,  
545 IASLC/ATS/ERS international multidisciplinary classification of lung adenocarcinoma novel concepts  
546 and radiologic implications. *Journal of Thoracic Imaging* **2012**, *27*, (6), 340-353.
- 547 31. Chen, G. L.; Feng, Q. Y.; Wang, J., Mini-review of microplastics in the atmosphere and their risks  
548 to humans. *Science of the Total Environment* **2020**, *703*, 135504.
- 549 32. Devesa, S. S.; Bray, F.; Vizcaino, A. P.; Parkin, D. M., International lung cancer trends by histologic  
550 type: male : female differences diminishing and adenocarcinoma rates rising. *International Journal of*  
551 *Cancer* **2005**, *117*, (2), 294-299.
- 552 33. Patel, J. D.; Bach, P. B.; Kris, M. G., Lung cancer in US women - a contemporary epidemic. *Jama-*  
553 *Journal of The American Medical Association* **2004**, *291*, (14), 1763-1768.
- 554 34. Schwabl, P.; Köppel, S.; Königshofer, P.; Bucsics, T.; Trauner, M.; Reiberger, T.; Liebmann, B.,  
555 Detection of various microplastics in human stool: a prospective case series. *Annals of Internal medicine*  
556 **2019**, *171*, (7), 453-457.
- 557 35. Ragusa, A.; Svelato, A.; Santacroce, C.; Catalano, P.; Notarstefano, V.; Carnevali, O.; Papa, F.;  
558 Rongioletti, M. C. A.; Baiocco, F.; Draghi, S., Plasticenta: first evidence of microplastics in human  
559 placenta. *Environment International* **2021**, *146*, 106274.
- 560 36. Allen, S.; Allen, D.; Phoenix, V. R.; Le Roux, G.; Jiménez, P. D.; Simonneau, A.; Binet, S.; Galop,  
561 D., Atmospheric transport and deposition of microplastics in a remote mountain catchment. *Nature*  
562 *Geoscience* **2019**, *12*, (5), 339-344.
- 563 37. Cai, L.; Wang, J.; Peng, J.; Tan, Z.; Zhan, Z.; Tan, X.; Chen, Q., Characteristic of microplastics in  
564 the atmospheric fallout from Dongguan city, China: preliminary research and first evidence.  
565 *Environmental Science Pollution Research* **2017**, *24*, (32), 24928-24935.
- 566 38. Dris, R.; Gasperi, J.; Rocher, V.; Saad, M.; Renault, N.; Tassin, B., Microplastic contamination in  
567 an urban area: a case study in Greater Paris. *Environmental Chemistry* **2015**, *12*, (5), 592-599.
- 568 39. Hours, M.; Fevotte, J.; Lafont, S.; Bergeret, A., Cancer mortality in a synthetic spinning plant in  
569 Besançon, France. *Occupational Environmental Medicine* **2007**, *64*, (9), 575-581.

- 570 40. Turcotte, S. E.; Chee, A.; Walsh, R.; Grant, F. C.; Liss, G. M.; Boag, A.; Forkert, L.; Munt, P. W.;  
571 Lougheed, M. D., Flock worker's lung disease: natural history of cases and exposed workers in Kingston,  
572 Ontario. *Chest* **2013**, *143*, (6), 1642-1648.
- 573 41. Donaldson, K.; Murphy, F.; Schinwald, A.; Duffin, R.; Poland, C. A., Identifying the pulmonary  
574 hazard of high aspect ratio nanoparticles to enable their safety-by-design. *Nanomedicine* **2011**, *6*, (1),  
575 143-156.
- 576 42. Tian, L.; Ahmadi, G., Fiber transport and deposition in human upper tracheobronchial airways.  
577 *Journal of Aerosol Science* **2013**, *60*, 1-20.
- 578 43. Kleinstreuer, C.; Feng, Y., Computational analysis of non-spherical particle transport and deposition  
579 in shear flow with application to lung aerosol dynamics—a review. *Journal of Biomechanical*  
580 *Engineering* **2013**, *135*, (2), 021008.
- 581 44. Shachar-Berman, L.; Ostrovski, Y.; De Rosis, A.; Kassinos, S.; Sznitman, J., Transport of ellipsoid  
582 fibers in oscillatory shear flows: implications for aerosol deposition in deep airways. *European Journal*  
583 *of Pharmaceutical Sciences* **2018**, *113*, 145-151.
- 584 45. Chow, A. H.; Tong, H. H.; Chattopadhyay, P.; Shekunov, B. Y., Particle engineering for pulmonary  
585 drug delivery. *Pharmaceutical Research* **2007**, *24*, (3), 411-437.
- 586 46. Lippmann, M.; Yeates, D.; Albert, R., Deposition, retention, and clearance of inhaled particles.  
587 *Occupational Environmental Medicine* **1980**, *37*, (4), 337-362.
- 588 47. Tran, C.; Buchanan, D.; Cullen, R.; Searl, A.; Jones, A.; Donaldson, K., Inhalation of poorly soluble  
589 particles. II. Influence of particle surface area on inflammation and clearance. *Inhalation Toxicology*  
590 **2000**, *12*, (12), 1113-1126.
- 591 48. Geiser, M.; Kreyling, W. G., Deposition and biokinetics of inhaled nanoparticles. *Particle Fibre*  
592 *Toxicology* **2010**, *7*, (1), 1-17.
- 593 49. Greim, H.; Borm, P.; Schins, R.; Donaldson, K.; Driscoll, K.; Hartwig, A.; Kuempel, E.; Oberdörster,  
594 G.; Speit, G., Toxicity of fibers and particles? Report of the workshop held in Munich, Germany.  
595 *Inhalation Toxicology* **2001**, *13*, (9), 737-754.
- 596 50. Kim, Y. I.; Kim, M. W.; An, S.; Yarin, A. L.; Yoon, S. S.; Interfaces, Reusable filters augmented  
597 with heating microfibers for antibacterial and antiviral sterilization. *ACS Applied Materials* **2020**, *13*, (1),  
598 857-867.
- 599 51. Liu, Y. H.; O'Brien, J. L.; Ajami, N. J.; Scheurer, M. E.; Amirian, E. S.; Armstrong, G.; Tsavachidis,

- 600 S.; Thrift, A. P.; Jiao, L.; Wong, M. C.; Smith, D. P.; Spitz, M. R.; Bondy, M. L.; Petrosino, J. F.;  
601 Kheradmand, F., Lung tissue microbial profile in lung cancer is distinct from emphysema. *American*  
602 *Journal of Cancer Research* **2018**, *8*, (9), 1775-1787.
- 603 52. Peters, B. A.; Hayes, R. B.; Goparaju, C.; Reid, C.; Pass, H. I.; Ahn, J., The microbiome in lung  
604 cancer tissue and recurrence-free survival. *Cancer Epidemiology Biomarkers & Prevention* **2019**, *28*,  
605 (4), 731-740.
- 606 53. Ren, Y.; Su, H.; She, Y.; Dai, C.; Xu, W., Whole genome sequencing revealed microbiome in lung  
607 adenocarcinomas presented as ground-glass nodules. *Translational Lung Cancer Research* **2019**, *8*, (3),  
608 235-246.
- 609 54. Parrish, K.; Fahrenfeld, N. L., Microplastic biofilm in fresh- and wastewater as a function of  
610 microparticle type and size class. *Environmental Science-Water Research & Technology* **2019**, *5*, (3), 495-  
611 505.
- 612 55. Emeville, E.; Giusti, A.; Coumoul, X.; Thome, J. P.; Blanchet, P.; Multigner, L., Associations of  
613 plasma concentrations of dichlorodiphenyldichloroethylene and polychlorinated biphenyls with prostate  
614 cancer: a case-control study in Guadeloupe (French West Indies). *Environmental Health Perspectives*  
615 **2015**, *123*, (4), 317-323.
- 616 56. Engel, L. S.; Zabor, E. C.; Satagopan, J.; Widell, A.; Rothman, N.; O'Brien, T. R.; Zhang, M. D.;  
617 Van Den Eeden, S. K.; Grimsrud, T. K., Prediagnostic serum organochlorine insecticide concentrations  
618 and primary liver cancer: a case-control study nested within two prospective cohorts. *International*  
619 *Journal of Cancer* **2019**, *145*, (9), 2360-2371.
- 620 57. Koutros, S.; Langseth, H.; Grimsrud, T. K.; Barr, D. B.; Vermeulen, R.; Portengen, L.; Wacholder,  
621 S.; Freeman, L. E. B.; Blair, A.; Hayes, R. B.; Rothman, N.; Engel, L. S., Prediagnostic serum  
622 organochlorine concentrations and metastatic prostate cancer: a nested case-control study in the  
623 Norwegian Janus serum bank cohort. *Environmental Health Perspectives* **2015**, *123*, (9), 867-872.
- 624 58. Park, E. Y.; Park, E.; Kim, J.; Oh, J. K.; Kim, B.; Hong, Y. C.; Lim, M. K., Impact of environmental  
625 exposure to persistent organic pollutants on lung cancer risk. *Environment International* **2020**, *143*,  
626 105925.
- 627 59. Gasperi, J.; Wright, S. L.; Dris, R.; Collard, F.; Mandin, C.; Guerrouache, M.; Langlois, V.; Kelly,  
628 F. J.; Tassin, B., Microplastics in air: are we breathing it in? *Current Opinion in Environmental Science*  
629 *Health* **2018**, *1*, 1-5.

- 630 60. Chen, Q. Q.; Reisser, J.; Cunsolo, S.; Kwadijk, C.; Kotterman, M.; Proietti, M.; Slat, B.; Ferrari, F.  
631 F.; Schwarz, A.; Levivier, A.; Yin, D. Q.; Hollert, H.; Koelmans, A. A., Pollutants in plastics within the  
632 North Pacific Subtropical Gyre. *Environmental Science & Technology* **2018**, *52*, (2), 446-456.
- 633 61. Wang, J. D.; Peng, J. P.; Tan, Z.; Gao, Y. F.; Zhan, Z. W.; Chen, Q. Q.; Cai, L. Q., Microplastics in  
634 the surface sediments from the Beijiang River littoral zone: composition, abundance, surface textures  
635 and interaction with heavy metals. *Chemosphere* **2017**, *171*, 248-258.
- 636 62. Asamoah, B. O.; Roussey, M.; Peiponen, K. E., On optical sensing of surface roughness of flat and  
637 curved microplastics in water. *Chemosphere* **2020**, *254*, 126789.
- 638 63. Paludan, S. R.; Reinert, L. S.; Hornung, V., DNA-stimulated cell death: implications for host  
639 defence, inflammatory diseases and cancer. *Nature Reviews Immunology* **2019**, *19*, (3), 141-153.
- 640 64. Whitehouse, D., Handbook of Surface and Nanometrology 2nd edn (Boca Raton, FL: CRC). **2011**.
- 641 65. Engineers, A. S. o. M., ASME B46. 1-2009: Surface Texture (Surface Roughness, Waviness, and  
642 Lay). **2009**.
- 643 66. Francisco, B.; Valentina, B.; Carmen, G.-B.; Mercedes, V., Cigarette butts as a microfiber source  
644 with a microplastic level of concern. *Science of The Total Environment* **2020**, 144165.
- 645 67. Catarino, A. I.; Macchia, V.; Sanderson, W. G.; Thompson, R. C.; Henry, T. B., Low levels of  
646 microplastics (MP) in wild mussels indicate that MP ingestion by humans is minimal compared to  
647 exposure via household fibres fallout during a meal. *Environmental Pollution* **2018**, *237*, 675-684.
- 648 68. Singh, R. P.; Mishra, S.; Das, A. P., Synthetic microfibers: pollution toxicity and remediation.  
649 *Chemosphere* **2020**, *257*, 127199.

650

## 651 **Acknowledgements**

652 We thank Professor Stefan HE Kaufmann (MPIIB, Berlin, Germany) for critical reading  
653 of the manuscript and insightful advice. We thank Jingjing Wang (Application Engineer  
654 of the Agilent Technologies, Shanghai, China) and Jinju Pei (Technical Engineer of the  
655 Agilent Technologies, Shanghai, China) for assistance with the *in situ* detection of  
656 microfibers in the lung slice. This project was supported by grants from the National  
657 Natural Science Foundation of China (81922030, 42077371 and 81770006 to H.L. and  
658 Q.C.). H. L. is sponsored by Projects supported by the National Science Foundation for  
659 Excellent Young Scholars of China (81922030), Shanghai ShuGuang Program

660 (20SG19), Shanghai Pujiang Program (16PJ1408600) and Shanghai Medical and  
661 Health Services Outstanding Youth Talent Program (2017YQ078).

662

### 663 **Author Contributions**

664 Q.C., C.C. and H.L. conceived the study and designed the experiments.

665 Q.C., J. G., H.L. analyzed the data and wrote the original draft.

666 H. H. reviewed and edited the manuscript.

667 H.Y. performed the microfiber separation and characterization.

668 Y. Y. carried out the SEM/EDS observation.

669 Y.Y. and Q. C. participated in the roughness measurement.

670 Q. C. and J.G. carried out the LDIR measurement together with Agilent Co.

671 J. G., H. S., Y. C., and Y. R. collected the clinical samples.

672

### 673 **Ethics declarations**

674 This study was conducted in accordance with the principles of the Declaration of  
675 Helsinki. The study protocol was approved by the ethics committee of the Shanghai  
676 Pulmonary Hospital (IRB NO. K21-020), and informed consent from individual  
677 patients was waived for this retrospective analysis.

### 678 **Competing interests**

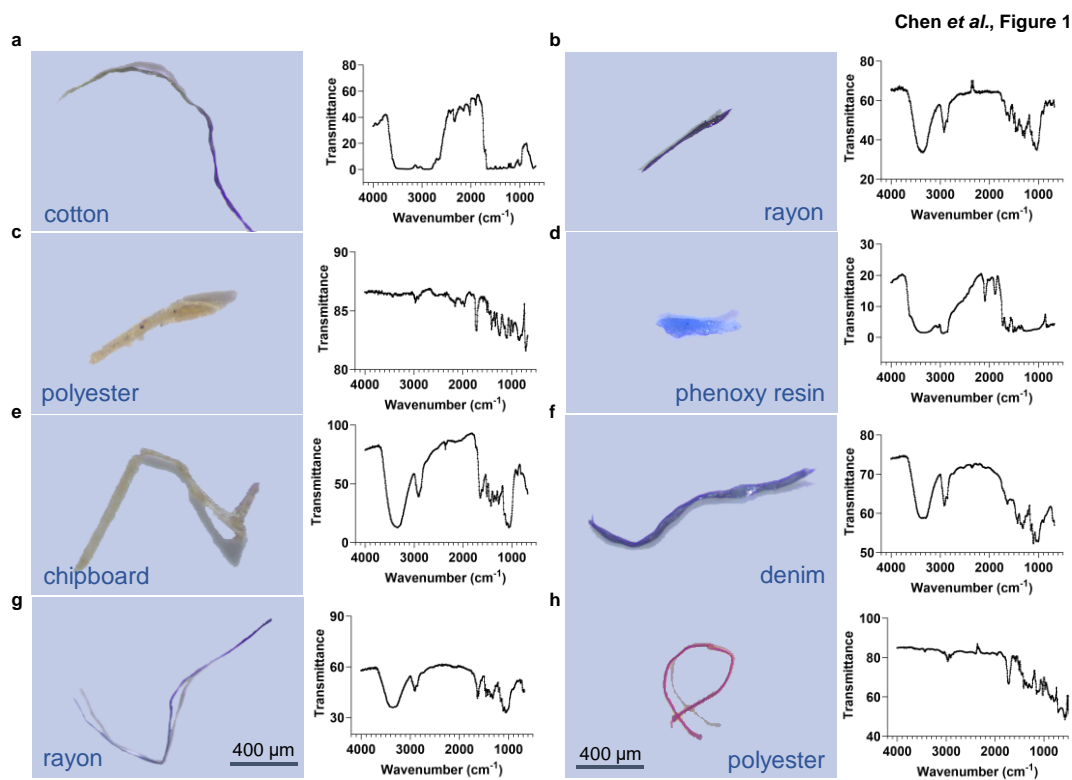
679 The authors declare no competing interests.

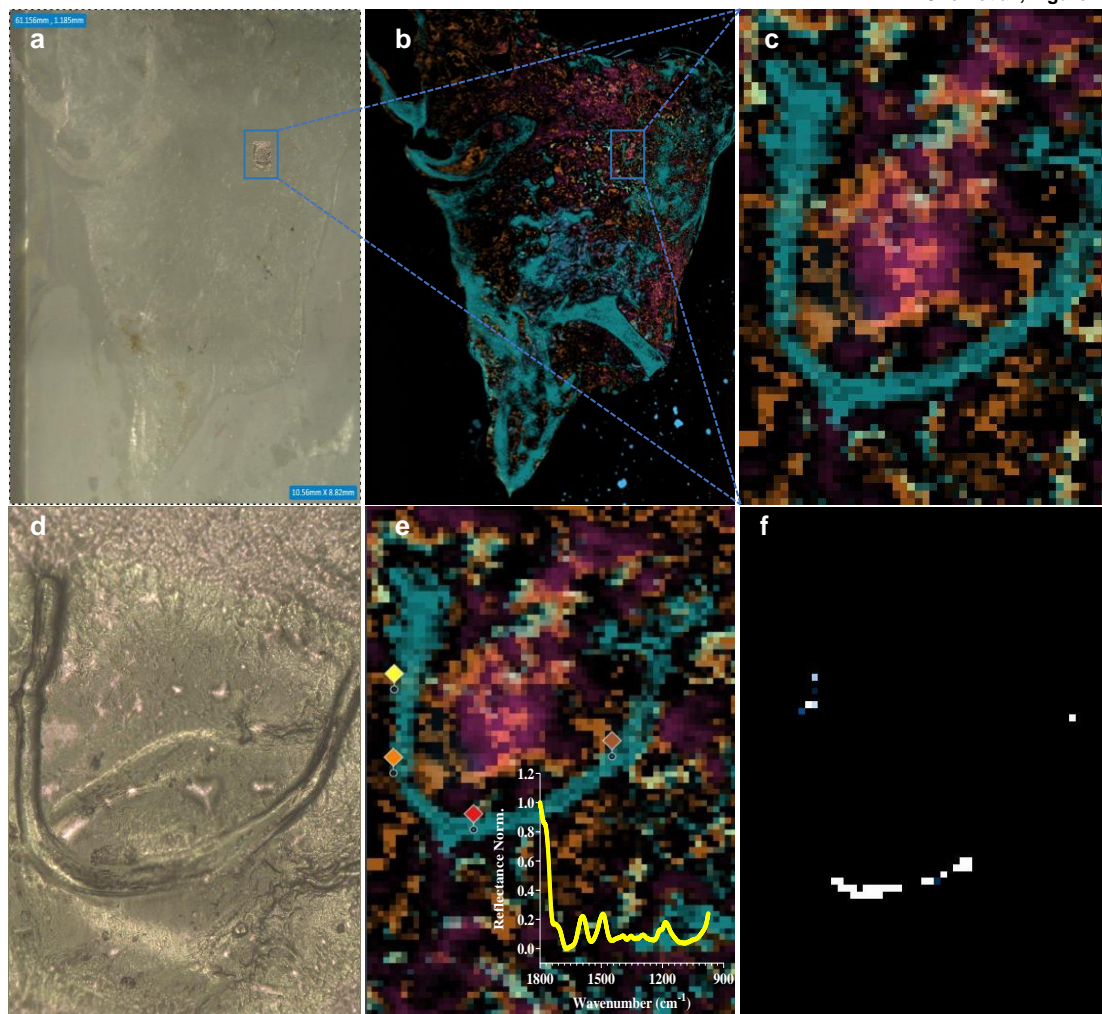
### 680 **Data availability**

681 The data are provided in the Figures and Supplementary Figures. Related information  
682 will be provided upon reasonable request.



683 **Figure Legends**





691

692 **Fig. 2** *In situ* detection of a cellulose microfiber in the tumor lung tissue slice. (a)

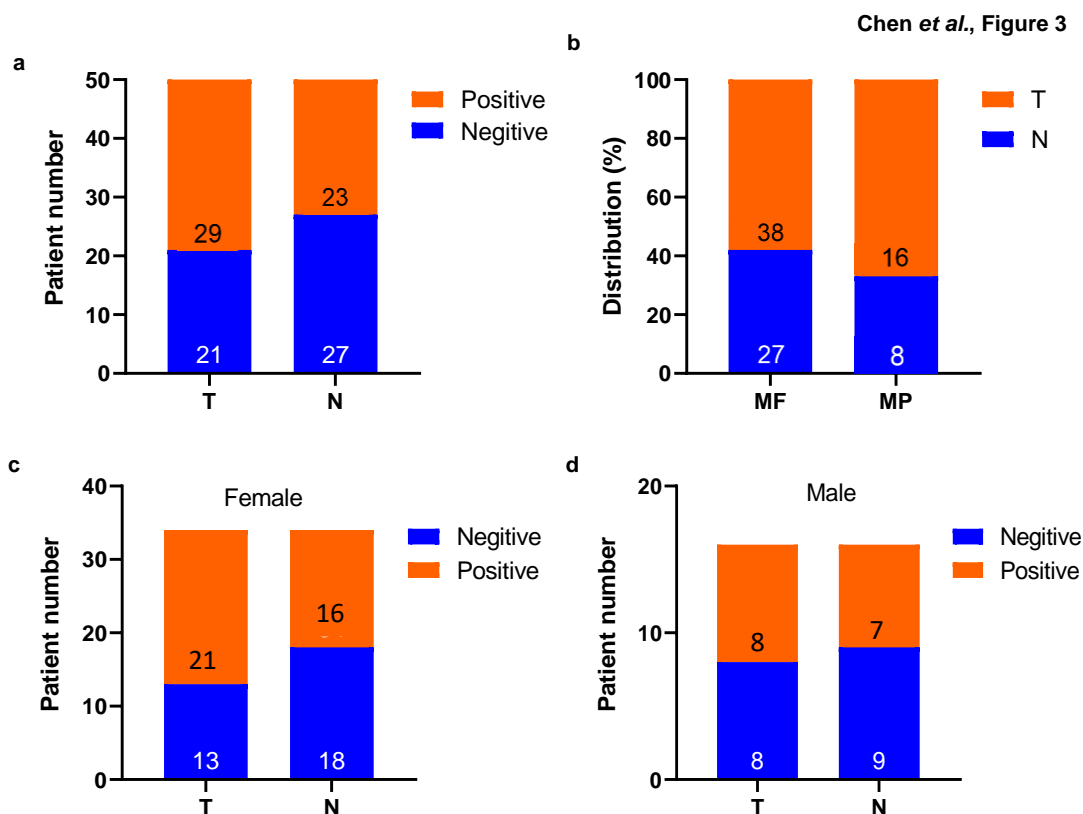
693 the whole tissue section image under vis-spectrum; (b) the whole tissue section image

694 under IR-spectrum; (c) microfiber detected under IR-spectrum; (d) microfiber detected

695 under vis-spectrum; (e) detected dots with confirmed cellulose composition; (f) strong

696 signals (in white color) with the specific cellulose characteristics.

697

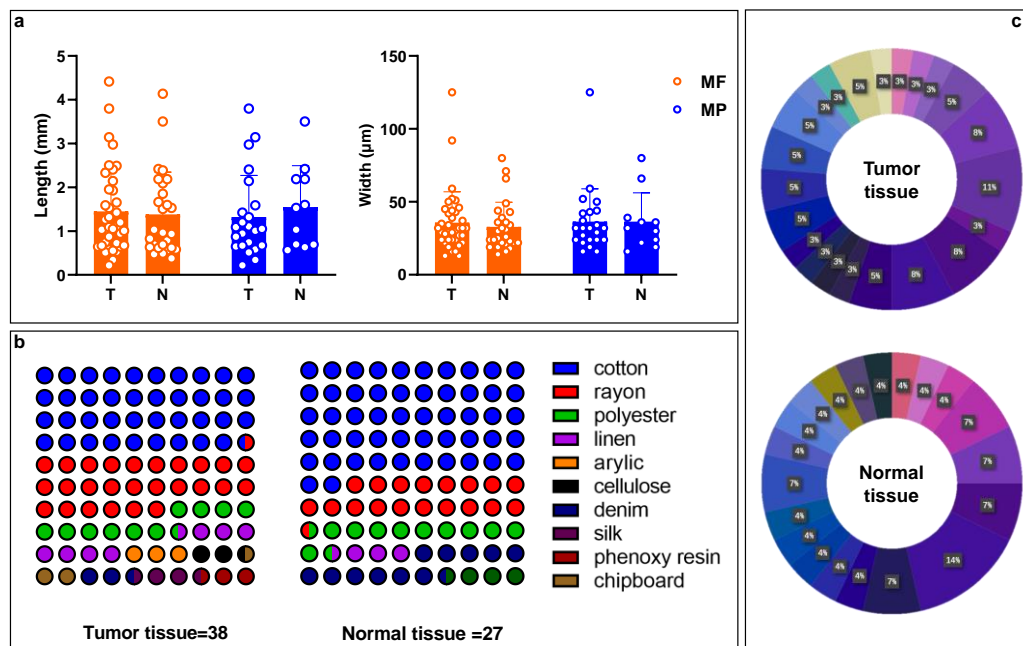


698

699 **Fig. 3 Microfiber and microplastic tissue distribution and detection frequency.** (a)  
700 Patient numbers with or without microfibers detected in lungs; (b) Distribution of  
701 microfibers and microplastics. T: tumor tissue; N: normal tissue; MF: microfiber; MP:  
702 microplastic; (c) Patient numbers with or without microfibers detected in women; (d)  
703 Patient numbers with or without microfibers detected in men. The annotated values on  
704 each bar of figures a, c, and d represent patient numbers; the annotated values on each  
705 bar of figure b represent detected microfiber or microplastic numbers.

706

Chen *et al.*, Figure 4



707

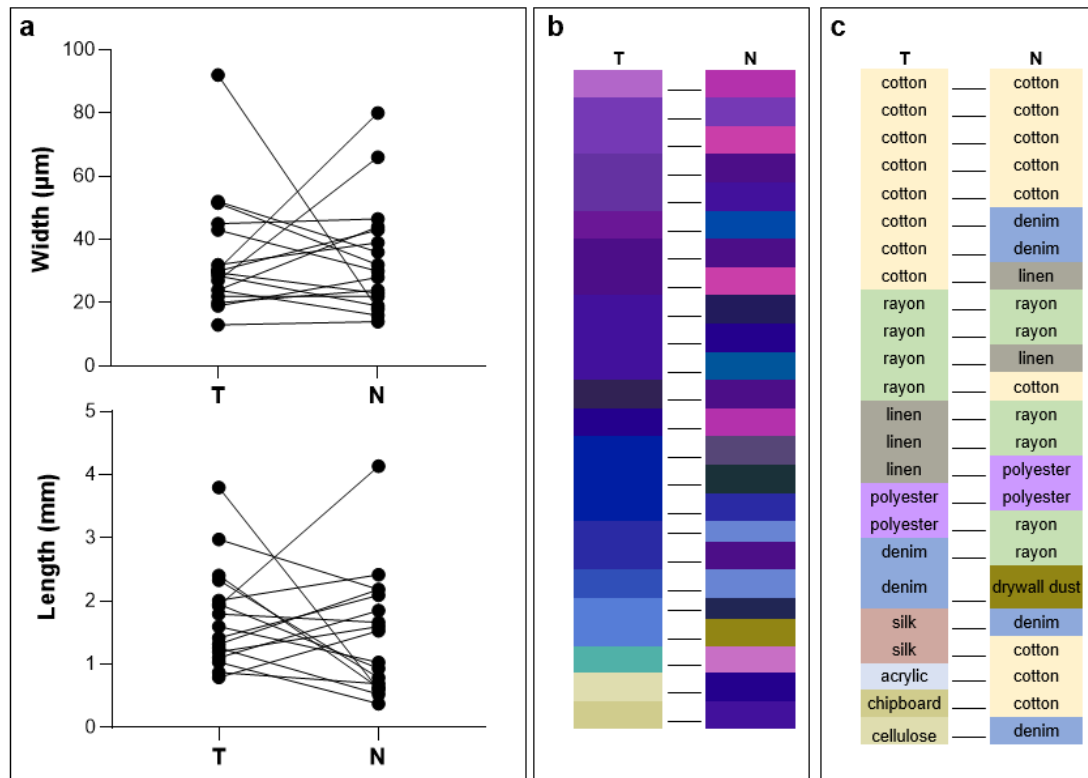
708 **Fig. 4 Microfiber characteristics in lung tumor and normal tissues.** (a) width and

709 length distribution; (b) composition type distribution (each dot represents 1% of the

710 total microfiber composition); (c) color distribution. T: tumor tissue; N: normal tissue.

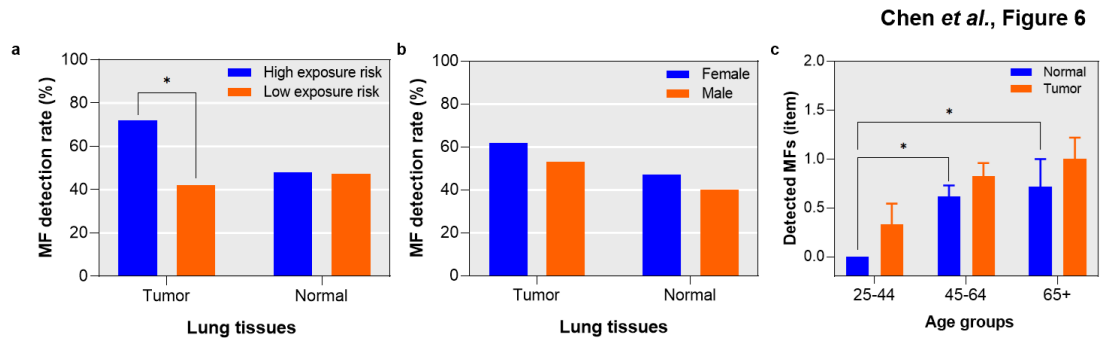
711 MF: microfiber; MP: microplastic.

Chen *et al.*, Figure 5



712

713 **Fig. 5 Microfiber characteristics in matched tumor/normal samples.** (a) width and  
714 length distribution; (b) color and composition type distribution. T: tumor tissue; N:  
715 normal tissue. Note: Only patients samples possessing microfibers in both tumor and  
716 adjacent normal tissue are included in this figure.

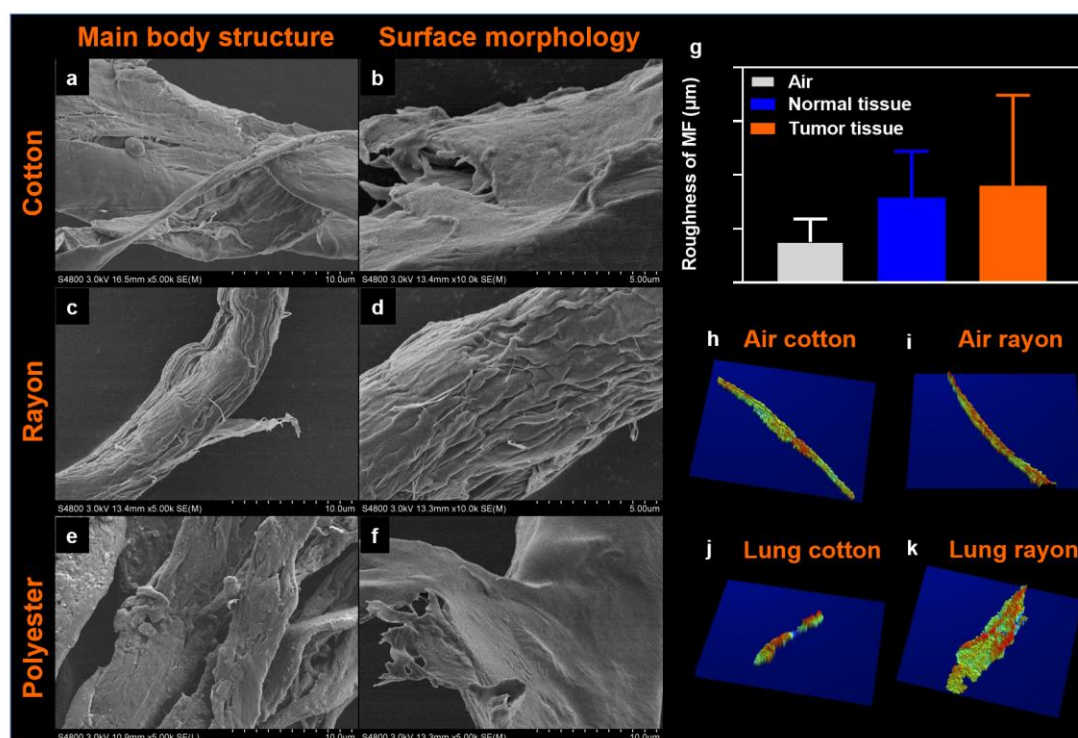


717

718 **Fig. 6 Correlation of microfibers with clinical indices** including (a) microfiber

719 exposure history; (b)gender; and (c) age.

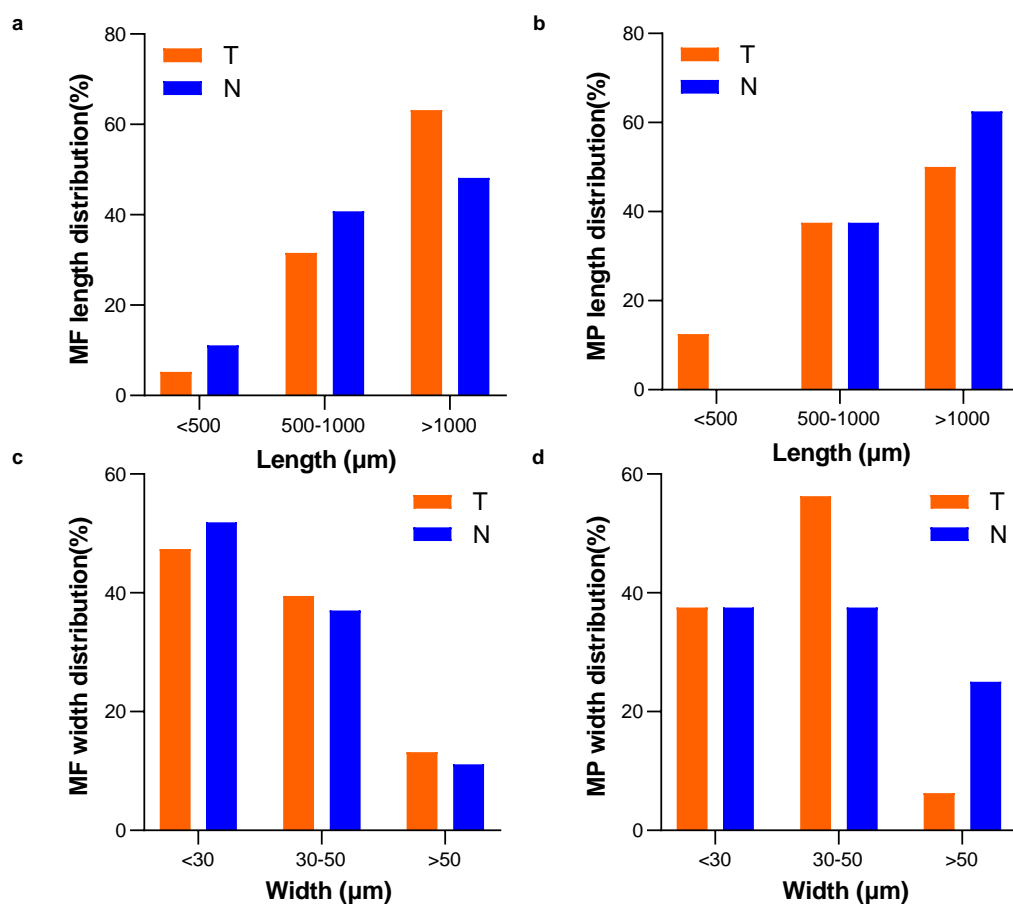
720



721

722 **Figure 7** Representative pictures of microfibers isolated from lung tissues under  
723 scanned electron microscope (SEM). (a) main body structure of cotton; (b) surface  
724 morphology of cotton; (c) main body structure of rayon; (d) surface morphology of  
725 rayon; (e) main body structure of polyester; (f) surface morphology of polyester; (g)  
726 the roughness value (Ra) for microfibers from air deposition, normal tissues and tumor  
727 tissues ( $n=4$  with 2 cotton microfibers, 1 rayon, and 1 polyester microplastics for each  
728 group according to their detected composition percentages); (h) representative surface  
729 roughness images for cotton microfiber from air deposition; (i) representative surface  
730 roughness images for polyester microplastic from air deposition; (j) representative  
731 surface roughness image for cotton microfiber from lung tissues; (k) representative  
732 surface roughness image for rayon microplastic from lung tissues.

Chen et al., Supplementary Figure 1

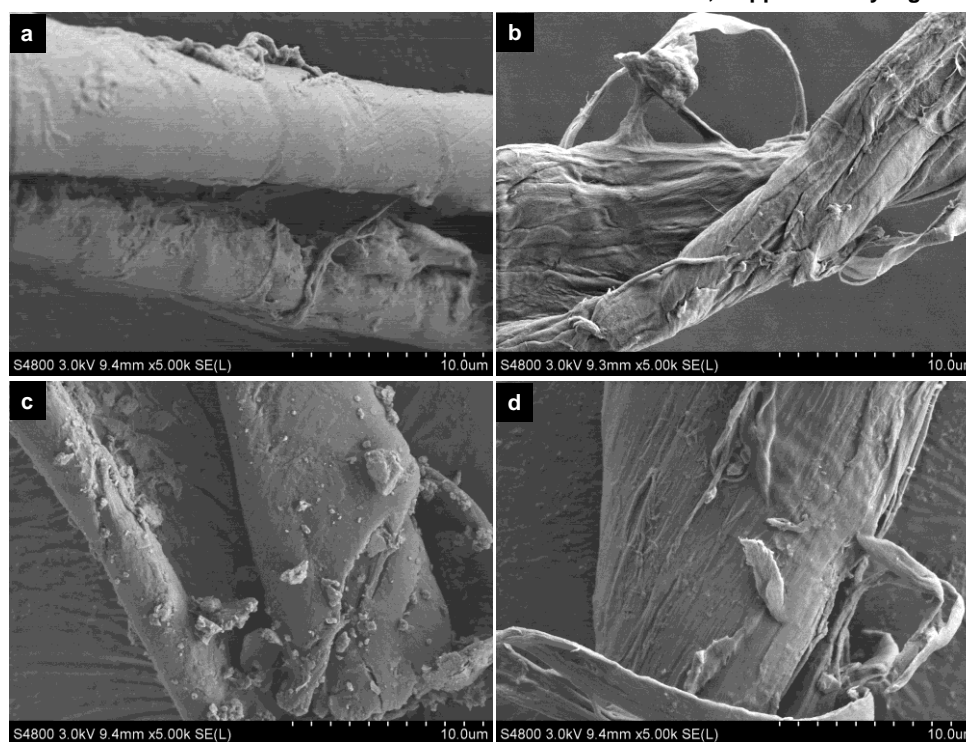


733

734 **Figure S1 Length and width distribution of microfibers and microplastics.** (a) the  
735 length distribution of microfibers; (b) the width distribution of microfibers; (c) the  
736 length distribution of microplastics; (d) the width distribution of microplastics. MF:  
737 microfiber; MP: microplastic.



Chen *et al.*, Supplementary Figure 2



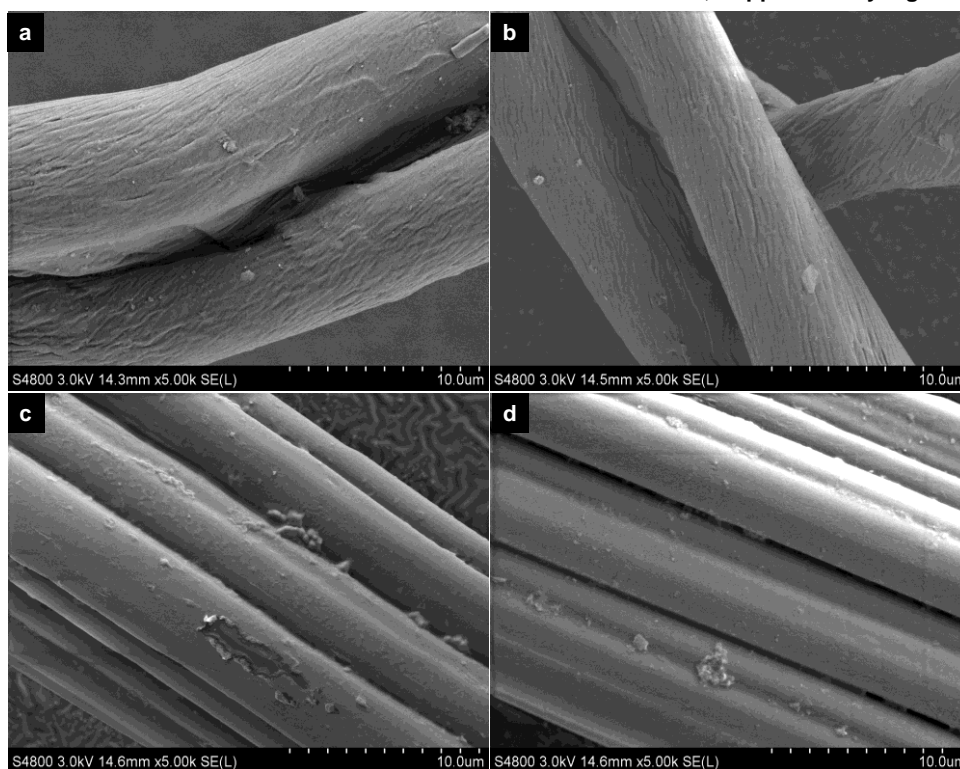
738

739 **Figure S2 Representative pictures of airborne cotton and rayon.** (a) cotton with

740 smooth surface; (b) cotton with rough surface; (c) rayon with smooth surface; (d) rayon

741 with rough surface.

Chen *et al.*, Supplementary Figure 3

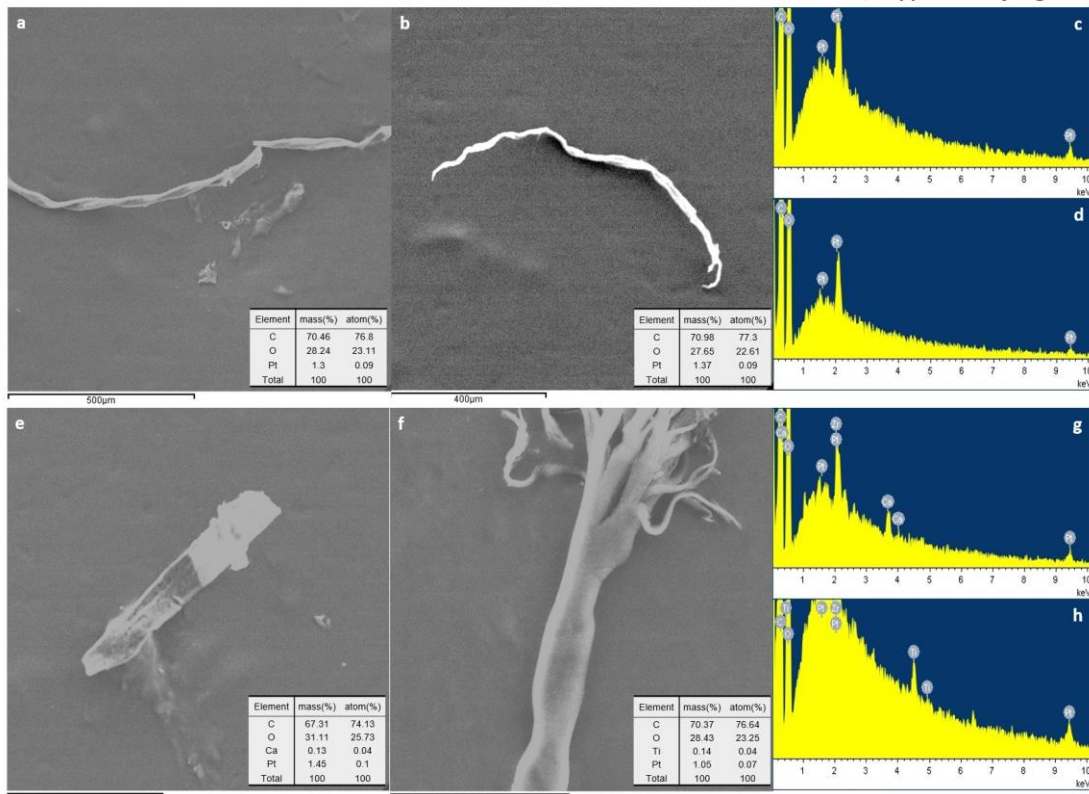


742

743 **Figure S3 Representative pictures of laboratory prepared cotton and rayon**  
744 **microfibers before and after experimental processes (digestion, observation, and**  
745 **identification).** (a) cotton before processes; (b) cotton after processes; (c) rayon before  
746 processes; (d) rayon after processes.

747

Chen et al., Supplementary Figure 4



748

749 **Figure S4 Microfiber surficial elemental composition illustrated by SEM/EDS. (a)**  
750 **cotton from a tumor tissue; (b) cotton from a normal tissue; (c) EDS figure for (a); (d)**  
751 **EDS figure for (b); (e) polyester from a tumor tissue; (f) polyester from a normal tissue;**  
752 **(g) EDS figure for (e); (h) EDS figure for (f).**

753

754 **Table 1. Clinical information of patients**

No.	Sex	Age range	Tobacco exposure	Cooking	Microfiber exposure	Risk assessment
1	Female	45-64	No	No	No	L
2	Male	45-64	No	No	No	L
3	Female	45-64	No	Yes	No	H
4	Female	NA	No	No	No	/
5	Female	45-64	No	No	Yes	H
6	Female	NA	No	No	No	/
7	Male	45-64	Yes	No	No	H
8	Female	45-64	No	No	No	L
9	Female	45-64	Yes	No	No	L
10	Male	45-64	Yes	No	No	H
11	Female	65+	No	No	No	L
12	Male	65+	Yes	No	Yes	H
13	Female	25-44	No	No	No	/
14	Male	45-64	Yes	No	Yes	H
15	Female	45-64	No	Yes	No	H
16	Female	65+	Yes	Yes	No	H
17	Female	45-64	No	Yes	No	H
18	Female	65+	No	No	No	/
19	Female	45-64	No	Yes	No	L
20	Female	65+	No	Yes	No	H
21	Female	45-64	No	Yes	No	H
22	Female	45-64	Yes	Yes	Yes	H
23	Male	45-64	Yes	No	No	H
24	Female	45-64	No	Yes	No	H
25	Female	45-64	No	No	No	/
26	Female	45-64	No	Yes	No	L

27	Male	45-64	No	No	No	L
28	Male	65+	Yes	No	Yes	H
29	Female	45-64	Yes	Yes	No	H
30	Female	45-64	Yes	Yes	Yes	H
31	Male	45-64	Yes	No	No	H
32	Female	45-64	Yes	Yes	No	H
33	Female	45-64	No	No	No	L
34	Male	45-64	No	No	No	L
35	Male	65+	Yes	No	Yes	H
36	Female	25-44	No	No	No	L
37	Female	45-64	No	No	No	L
38	Female	45-64	Yes	Yes	No	H
39	Male	45-64	Yes	No	No	H
40	Male	45-64	No	No	No	L
41	Male	25-44	No	No	No	L
42	Female	45-64	No	No	No	L
43	Male	45-64	Yes	No	Yes	H
44	Female	25-44	Yes	Yes	No	L
45	Female	45-64	No	Yes	No	H
46	Female	25-44	Yes	Yes	No	L
47	Female	25-44	No	No	No	L
48	Female	45-64	No	No	No	L
49	Female	45-64	No	Yes	Yes	H
50	Male	45-64	No	No	No	L

755

756

757 **Table 2. Characteristics of patients**

<b>Characteristic</b>	<b>Patients(n=50)</b>
Female sex (n, %)	34 (68.0)
Age (mean $\pm$ SD) (y)	55.4 $\pm$ 10.1
History of diabetes (n, %)	4 (8.0)
Hypertension (n, %)	13 (26.0)
COPD (n, %)	0 (0)
Coronary artery disease (n, %)	2 (4.0)
Stroke (n, %)	1 (2.0)
Pulmonary embolism (n, %)	0 (0)
History of tobacco exposure (n, %)	19 (38.0)
Adjuvant chemotherapy (n, %)	1 (2.0)
Adjuvant radiotherapy (n, %)	0 (0)
Neoadjuvant therapy (n, %)	0 (0)
Adjuvant Target therapy (n, %)	0 (0)
Surgical laterality (n, %)	
Left	18 (36.0)
Right	32 (64.0)
Intrapericardial Procedure	
Yes	0 (0)
No	50 (100)

758 *COPD: chronic obstructive pulmonary disease.*